

Development of a Seismometer-Type Absolute Displacement Sensor Aimed at Detecting Earthquake Waves with a Large Magnitude and Long Period

Kazuto Seto¹, Yuichi Iwasaki², Akihiko Itoh³ and Ikuo Shimoda⁴

1. *Seto-Vibration Control Laboratory, Kanagawa 240-0116, Japan*

2. *Engineering and Design Department, Oiles Co., Tochigi 326-0327, Japan*

3. *Research and Development Department, Oiles Co., Kanagawa 252-0811, Japan*

4. *Oiles Co., Tokyo 108-0075, Japan*

Abstract: This paper proposes a novel seismometer-type absolute displacement sensor aimed at detecting earthquake waves with a large magnitude and long period. However, since the measuring range of the displacement sensor is higher than its natural frequency, it is difficult to detect low frequency vibrations below 1 Hz using a conventional seismic-type displacement sensor. In order to provide an absolute displacement detection which is capable of lowering the natural frequency and enlarging the detectable amplitude without causing structural defects, the relative signals of displacement, velocity, and acceleration between a detected object and the auxiliary mass of the sensor are fed back into the sensor. In addition, phase lag compensation is inserted to adjust phase angles, which are of a frequency of 1 Hz. According to simulation results, a detection range from 0.1 Hz to 50 Hz is expected. It has been demonstrated that the developed sensor with a small size and light weight has a detection range of from 0.5 Hz to 50 Hz for absolute displacement and velocity. As an additional advantage, the measurement displacement amplitude has been expanded to about 20 dB. This sensor is available to use for the active control of flexible structures like high rise buildings using the LQ control method.

Key words: Vibration, displacement sensor, earthquake wave, measurement, structural control.

1. Introduction

Recently, active control systems have been widely applied in vibration control of civil structures [1]. Active control systems require dynamic information of the structure, such as absolute displacement and velocity [2]. Generally, a seismometer-type sensor is used to measure such information. The three kinds of seismometer-type sensors are acceleration, velocity and displacement sensors [3, 4]. For obtaining an absolute displacement signal using the two former types, it is necessary to use integrators, however, a drift problem in the integrator happens at times. Therefore high-performance integrators are required

to reduce the drift problem. Our interest is in the latter sensor type to directly measure the absolute displacement of structures, especially frequency ranges below 1 Hz [5]. However, it is difficult to measure such low frequency vibration using conventional seismic-type sensors [6], because the measurement range of the absolute displacement is above the natural frequency of the sensor. To reduce the natural frequency, the sensor needs a larger mass and softer springs. However, these modifications make the sensor larger and more fragile against vibrations.

This paper proposes an absolute displacement sensor with a feedback control loop and a phase compensator, in order to expand the measuring-frequency range to lower frequencies. The

Corresponding author: Kazuto Seto, PhD, research fields: vibration control and modeling. E-mail: sseto@seto-vcl.com.

sensitivity of the sensor at lower frequencies is enhanced by using feedback from the relative displacement, velocity, and acceleration signals between the measured object and the internal weight of the sensor [7]. The positive feedback from the relative displacement is equivalent to adding a negative spring constant. The negative feedback from the relative acceleration virtually increases the internal weight. Subsequently, this can make the natural frequency of the sensor lower without additional weight as well as soften the spring. The relative velocity feedback is equivalent to adding a negative or positive damping effect. Therefore, it is possible to adjust the damping ratio to a desired value using this feedback. Moreover, it is also possible to increase the measurable maximum amplitude of the sensor, because the feedback suppresses displacement of the internal weight.

In this study, a prototype sensor with a feedback control loop was built. A moving coil attached to the internal weight measured the relative velocity signal. The relative displacement is obtained by integration of the relative velocity, while the relative acceleration is obtained as a derivative. In addition, phase lag compensation is inserted to adjust phase angles, which are below a frequency of 1 Hz. It has been demonstrated that the developed sensor with a small size and lightweight has a measurement range of from 0.5 Hz to 50 Hz for absolute displacement and velocity.

2. Proposed Sensor

2.1 Construction of the Proposed Sensor

This sensor consists of a sensor body, a control circuit and a phase compensator as shown in Fig. 1. The sensor body, which belongs to a type of seismic sensor, is made up of an internal weight with a mass, m , a couple of spring units with a spring constant, k , a damping element with a damping constant, c , an actuator to generate a control force, f_c , and a velocity detector to detect relative velocity, $(\dot{u} - \dot{x})$.

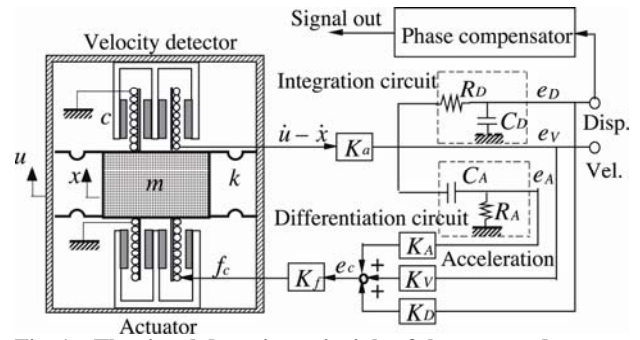


Fig. 1 The signal detection principle of the proposed sensor.

The spring unit supports the internal weight in order to move smoothly in the x direction.

The control circuit is composed of a signal translation amplifier with the gain constant, K_o , an integration circuit with time constant, $T_D = C_D R_D$, a differential circuit with time constant, $T_A = C_A R_A$, and a signal adder and feedback gain adjusters. A relative velocity signal, e_V , translated from the relative velocity, $(\dot{u} - \dot{x})$, through the signal translation amplifier is adapted to generate relative displacement and acceleration signals, e_D and e_A , respectively. Three signals of relative displacement, velocity and acceleration multiplied by displacement, velocity and acceleration feedback gains, K_D , K_V and K_A , respectively, are used to generate a control signal. The control signal, e_C , added to the three signals produces the control force, f_c , through an amplifier with gain constant, K_f . Since the integration circuit is included in the feedback loop, the drift problem caused by signal integration does not happen. A phase compensator was adapted to compensate the phase angle for expansion of the measurement range to a frequency lower than 1 Hz. This will be explained in detail later.

2.2 Frequency Transfer Function

When all feedback gain becomes negative as in Fig. 1, the transfer function between an absolute displacement of the measured object, u , and the relative displacement signal, e_D , is obtained as:

$$\frac{e_D}{u} = \frac{mK_a(T_{AS}+1)s^3}{a_0s^4 + a_1s^3 + a_2s^2 + a_3s + a_4} \quad (1)$$

Also, the transfer function between an absolute displacement of the measured object u and the relative velocity signal, e_v , is obtained as:

$$\frac{e_v}{u} = \frac{mK_a\{T_D T_A s^2 + (T_D + T_A)s + 1\}s^3}{a_0 s^4 + a_1 s^3 + a_2 s^2 + a_3 s + a_4} \quad (2)$$

where the coefficients of each denominator are:

$$\begin{aligned} a_0 &= T_D T_A m \\ a_1 &= (T_D + T_A)m + T_D T_{AC} + T_D T_A K_a K_f (K_A + K_V) \\ a_2 &= m + (T_D + T_A)c + T_D T_A k + T_A K_a K_f (K_V + K_D + K_A) \\ a_3 &= (T_D + T_A)k + c + K_a K_f (K_D + K_V) \\ a_4 &= k \end{aligned}$$

The transfer function of the differential circuit shown in Fig. 1 is as follows:

$$G(s) = \frac{T_A s}{T_A s + 1} \quad (3)$$

The transfer characteristic of Eq. (3) can be approximated by Eq. (4), when the denominator of Eq. (3) takes the form of $T_A s + 1 \approx 1$ if $T_A s \ll 1$.

$$G(s) = T_A s \quad (4)$$

Meanwhile, the transfer function of the integration circuit shown in Fig. 1 is as follows:

$$G(s) = \frac{1}{T_D s + 1} \quad (5)$$

The transfer characteristic of Eq. (5) can be approximated by Eq. (6), when $T_D s + 1 \approx T_D s$ if $T_D s \gg 1$.

$$G(s) = \frac{1}{T_D s} \quad (6)$$

Then, the transfer function of Eq. (7) is obtained from Eq. (1) to (6) as follows:

$$\frac{e_D}{u} = \frac{mK_a s^2}{T_D(m + T_A K_a K_f K_A)s^2 + T_D(c + K_a K_f K_V)s + T_D k + K_a K_f K_D} \quad (7)$$

Therefore, the natural frequency, ω_n , and the damping ratio ζ are derived as follows:

$$\omega_n = \sqrt{\frac{(k + \frac{1}{T_A} K_a K_f K_D)}{(m + T_A K_a K_f K_A)}} \quad (8)$$

$$\zeta = \frac{c + K_a K_f K_V}{2\sqrt{(m + T_A K_a K_f K_A)(k + \frac{1}{T_D} K_a K_f K_D)}} \quad (9)$$

2.3 Effects of Each Feedback

Effects of each feedback are observed from Eqs. (8) and (9).

- Relative displacement feedback:

Using feedback from the relative displacement signal changes the equivalent spring constant of the sensor. Using positive feedback of the relative displacement can reduce the spring constant and lowers the natural frequency of the sensor. This is because a polarity of the displacement feedback gain, K_D , changes from + to - pole in Eq. (8).

- Relative velocity feedback:

Using relative velocity feedback changes the equivalent damping coefficient of the sensor. The damping coefficient becomes smaller from using positive feedback of the relative velocity, but becomes larger using negative feedback.

- Relative acceleration feedback:

The equivalent mass of the sensor is changed by the relative acceleration feedback. Negative feedback of the relative acceleration reduces the natural frequency of the sensor. Meanwhile, the damping ratio of the sensor becomes larger by using positive feedback and smaller by using negative feedback.

2.4 Additional Effects of Relative Acceleration Feedback

In addition, negative feedback of the relative acceleration can expand the measurement range of the displacement. The transfer function between the absolute displacement of the measured object, u , and the relative displacement, $(u-x)$, is:

$$\frac{u-x}{u} = \frac{mT_D s^2}{(m + T_A K_a K_f K_A)s^2 + T_D(c + K_a K_f K_V)s + T_D k + K_a K_f K_D} \quad (10)$$

The measurement range of this sensor lies in a higher frequency domain than the natural frequency of the sensor. Therefore, the transfer characteristic of Eq. (10) can be approximated as:

$$\frac{u-x}{u} \approx \frac{m}{m + T_A K_a K_f K_A} \quad (11)$$

Hence, the relative displacement amplitude of the auxiliary mass h can be denoted as:

$$u - x = h = \frac{m}{m + T_A K_a K_f K_A} u \quad (12)$$

In Eq. (12), the coefficient of u becomes lower if a negative K_A feedback is applied. This means the relative displacement can be suppressed by adding K_A , and the maximum measurable displacement amplitude can be expanded.

3. Simulation

Main dimensions of the prototype sensor are as follows:

$$m = 25.2 \text{ [g]}, \quad c = 5.23 \text{ [Ns/m]}, \quad k = 30.1 \text{ [N/m]}.$$

Using these dimensions and the transfer function shown in Eq. (7), an example of simulation results is shown in the left side of Fig. 2, where the dotted and solid lines indicate the frequency responses of the original (non-feedback) system and all feedback (positive displacement gain of $K_D = 220$, negative acceleration gain of $K_A = -220$ and negative velocity gain of $K_D = 0.5$) controlled system, respectively. This figure shows that the natural frequency located at 5.5 Hz of the original system was moved to 0.68 Hz with a damping factor of $\zeta = 0.4$ using the all feedback system.

Although it is possible to move the natural frequency lower using the all feedback system, another way is introduced in order to expand the measurement range to an even lower frequency. This method is to use a phase lag compensator [8], since the phase angle leads to a positive degree under the natural frequency. The transfer function of the second order of the phase lag compensator is expressed as:

$$G_c(s) = \frac{s^2 + 2\zeta_n \omega_n s + \omega_n^2}{s^2 + 2\zeta_d \omega_d s + \omega_d^2} \quad (13)$$

$$\omega_n = 0.68 \times (2\pi) \text{ [rad/s]}, \quad \zeta_n = 0.35$$

$$\omega_d = 0.2 \times (2\pi) \text{ [rad/s]}, \quad \zeta_d = 0.4$$

By selecting the natural frequency, $\omega_n = 0.68 \times 2\pi$, and damping factor, $\zeta_n = 0.4$, to cancel out the

natural frequency and damping factor of the all feedback controlled system, the frequency response of the above-transfer function of the second order of the phase lag compensator is shown in Fig. 3.

Fig. 4 shows the effectiveness of the all feedback controlled system with the above mentioned gains and the phase lag compensation for seismic type proposed sensor. Notable points in Fig. 4 are the drop in gain from 0 dB to -20 dB and the shifting in the corresponding natural frequency from 5.5 Hz to 0.2 Hz. This gives a possibility for realizing an absolute displacement sensor to measure seismic waves with a long period and large amplitude, nevertheless using a small size sensor.

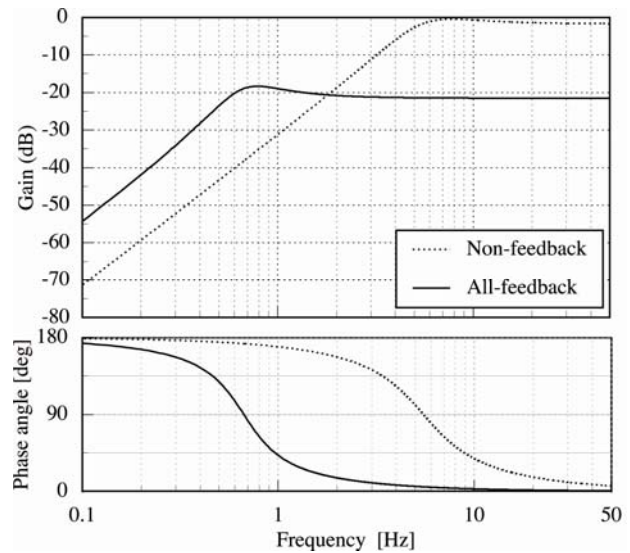


Fig. 2 Effectiveness of all feedback control with displacement, velocity and acceleration.

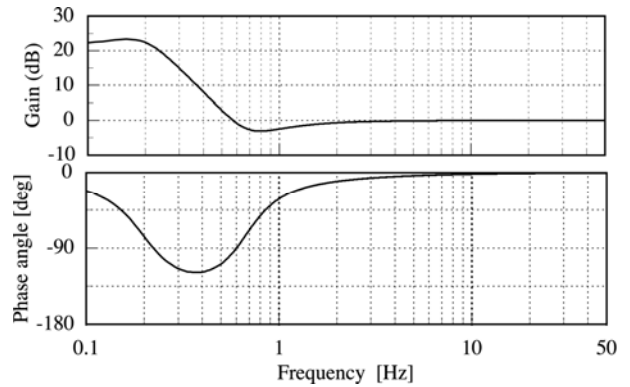


Fig. 3 Frequency response of corresponding phase lag compensator.

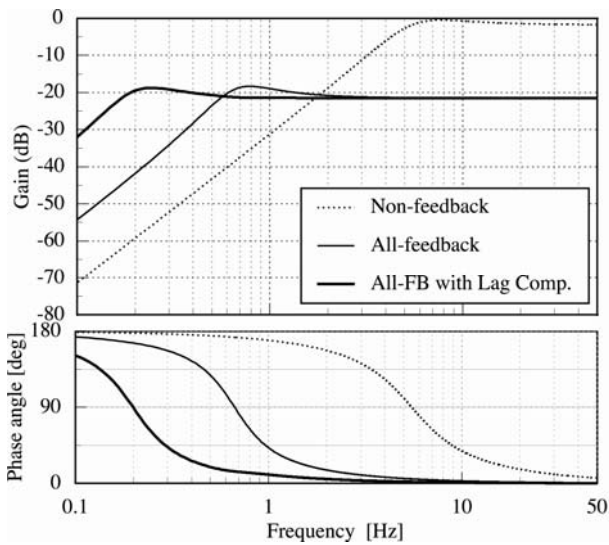


Fig. 4 Effectiveness of phase lag compensation for the proposed seismic type sensor with all feedback control.

Regarding the aim of a small-sized sensor, it was demonstrated that negative acceleration feedback is effective in expanding the measurement range. The thin solid line in Fig. 5 shows a frequency response for the proposed seismic-type sensor with negative acceleration feedback. Effectiveness of the phase-lag compensation for the proposed seismic-type sensor with negative acceleration feedback is demonstrated by the frequency response expressed by the thick line. The natural frequency located at 5.5 Hz in the case of the original system was shifted to 0.6 Hz by the use of the negative acceleration feedback and was shifted still more to 0.1 Hz by phase-lag compensation. Furthermore, it is important to notice that the gain in the measurement range was expanded from 0 dB = 1 in the original system to -40 dB = 1/100 by use of the negative acceleration feedback. This means that the measurement range of the sensor was expanded by about 100 times, and a small-size sensor with 1mm of moving distance was able to measure 100 mm of the absolute displacement of a measured object. If such a seismometer-type absolute displacement sensor is realized, it will be possible to detect earthquake waves with a large magnitude and long period. This is the design target of developing the seismometer-type absolute displacement sensor with dynamic characteristics as shown in Fig. 5.

4. Experiment

Fig. 6 shows a sketch of the experimental setup of the measurement system composed of an electromagnetic shaker, a shaker amplifier, a TF (Transfer Function) analyzer and a sensor control board with feedback controller and a phase lag compensator. The proposed sensor was attached to the electromagnetic shaker. A laser sensor was used to measure the input signal to the sensor. The TF analyzer obtained the frequency response between the laser sensor signal and the signal of the proposed sensor.

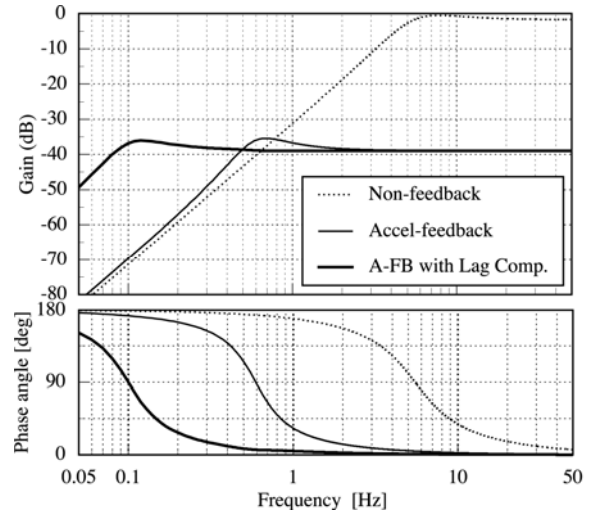


Fig. 5 Design target of developing a seismometer-type absolute displacement sensor.

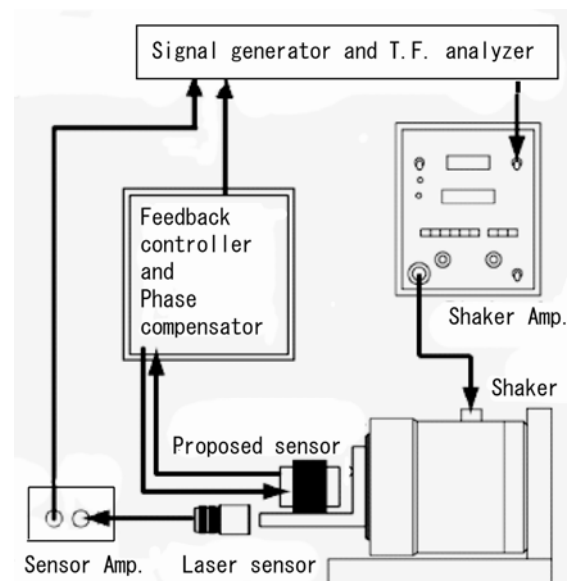


Fig. 6 Measurement system of the frequency response of the sensor.

4.1 Experimental Results

Fig. 7 shows an example of the experimental results of the frequency response between the laser sensor signal and the output signal from the proposed sensor. All feedback gains of K_A , K_D , and K_D were determined to obtain the corresponding frequency response shown in Fig. 2. The damping ratio was adjusted by selecting a suitable value for the relative velocity. Taking the above items into consideration, the natural frequency was shifted from 5.5 Hz to 0.7 Hz with a damping factor of $\zeta = 0.4$ by all feedback. As a result, the prototype sensor with a measuring frequency range from about 0.8 Hz (frequency shifted into 90° at phase angle) to 50 Hz, as shown by the solid line, was attained. As an additional advantage, the measurement displacement amplitude was expanded to about 20 dB. Comparing Fig. 7 to Fig. 2, the experimental results agree well with the simulation results over the natural frequency of 0.7 Hz, however, differences in the gain and phase angle come out under the natural frequency gradually.

Fig. 8 shows the experimental result corresponding to the simulated results shown in Fig. 4. Although the phase lag compensation was added, the frequency response indicated by the thick solid line was not improved at the low frequency range of under 0.5 Hz. A problem, which occurred in the lower frequencies, will be improved by magnetic shielding from the electromagnetic shaker to the sensor, because the effect of an electromagnetic wave induced from the shaker to the sensor is very sensitive under a lower frequency range with a feeble signal. If the frequency response of the phase angle is 180° below 1 Hz, it is possible to realize the frequency response indicated by the thick line in Fig. 4.

The frequency response of the developed absolute displacement sensor with the best adjustment in this stage is shown by a thick solid line in Fig. 8. The natural frequency located at 5.5 Hz in the case of the original system was shifted to 0.5 Hz by the use of the adaptable feedback control system and phase-lag

compensation. This frequency response corresponds to a second order high-pass filter system with $\omega_n = 0.5 \times 2\pi$ and $\zeta = 0.4$, as shown in Fig. 9.

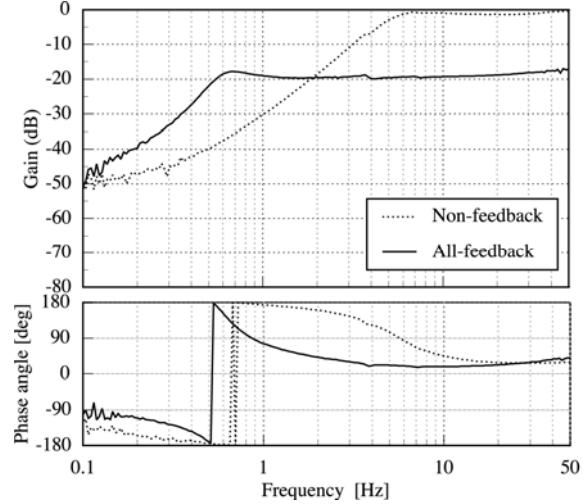


Fig. 7 Measured frequency response of the developed sensor with all types of feedback corresponding to the simulation result shown in Fig. 2.

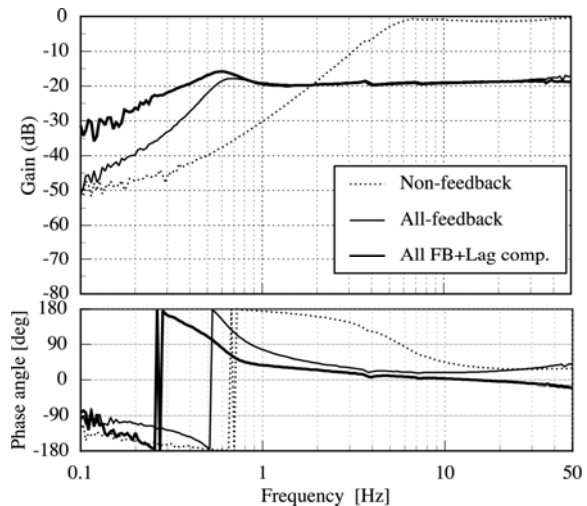


Fig. 8 Measured frequency responses of the developed sensor compensated by phase-lag corresponding to Fig. 4.

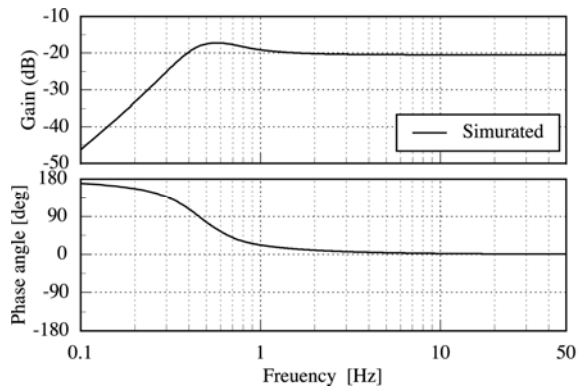


Fig. 9 Frequency response of a second order high-pass filter system with $\omega_n = 0.5 \times 2\pi$ and $\zeta = 0.4$.

5. Application Examples

Since the developed absolute displacement sensor can observe low frequency vibrations below 1 Hz, there are various application fields, such as seismic observations, active vibration controls for flexible structures, and active isolations [9] from lower frequency disturbance.

5.1 Seismic Observation

As the typical application example of the developed absolute displacement sensor, two kinds of observation waves based on a Kobe wave and a Hachinohe wave are used. As is well known, the dominant frequency is located at about 1 Hz in the case of a Kobe wave, and about 0.3 Hz in the case of a Hachinohe wave. Therefore, it seems to be better to test the observation performance of the sensor using the two seismic waves.

Fig. 10 shows the comparison of the ground motion based on a Kobe wave and its observed motion using the second order high pass filter system indicated in Fig. 9. The dotted line shows the ground motion and the solid line is of the observed motion expanded 10 times, because the observed signal is condensed to one-tenth. It seems that the Kobe wave can be observed well using the developed sensor.

In compared with Fig. 10, the observed motion of a Hachinohe wave, shown in Fig. 11, is relatively coincident on the amplitude, although the phase is shifted forward. Since it is important to measure the amplitude of displacement exactly in a seismic observation system, it may be applicable to this system.

When the design target of the seismometer-type absolute displacement sensor shown by the thick line in Fig. 5 is realized, the observed motion of the Hachinohe wave shown in Fig. 11 is improved as shown in Fig. 12. It seems that the Hachinohe wave is observed well using the developed sensor with measuring frequency range over 0.1 Hz. This is possible to realize the design target by replacing a

shaker from the electromagnetic type to a hydraulic one, in order to isolate an electromagnetic wave induced to the sensor coil. It will be shown by next paper.

5.2 Active Vibration Controls for a Model Structure with a Low Natural Frequency

In recent years, the numbers of newly built three-story houses in Japan has been on the rise in urban areas in order to maximize living spaces within smaller housing areas. These houses are subject to problems caused by traffic vibrations, because the dominant frequency of the traffic vibration located at

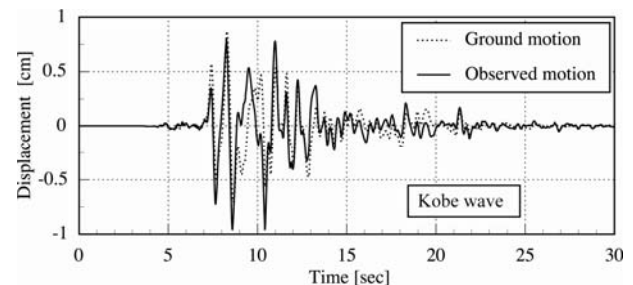


Fig. 10 Comparison of the ground motion based for a Kobe wave and its observed motion using the second order high pass filter system indicated in Fig. 9.

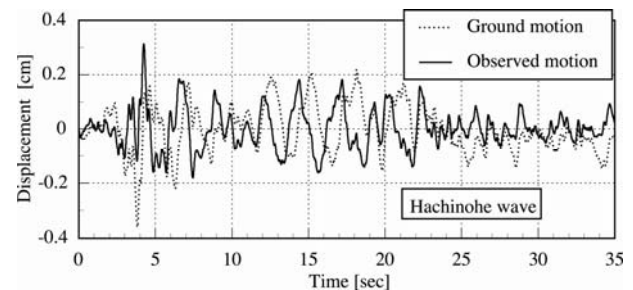


Fig. 11 Comparison of the ground motion based for a Hachinohe wave and its observed motion using the second order high pass filter system indicated in Fig. 9.

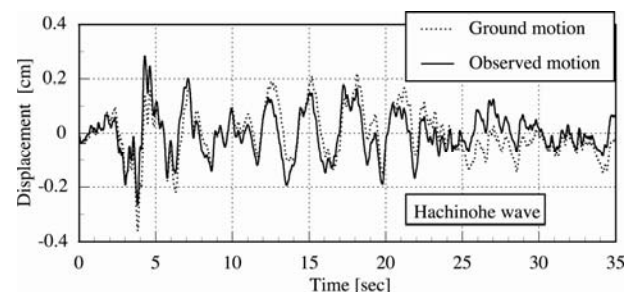


Fig. 12 Comparison of the ground motion based on a Hachinohe wave and its observed motion when the design target of the seismometer-type absolute displacement sensor is realized.

about 3 Hz is coincident with the natural frequency of these houses. Although TMD (tuned mass dampers) are considered to solve the problem, they require a heavy auxiliary mass on the top floor in order to obtain effective vibration-reduction [10]. Such masses can result in increased danger caused by large earthquakes. As an effective method, AMD (active mass dampers) are well known to control the vibration of high-rise buildings and huge bridge tower [11] vibrations caused by wind excitation. In this research, the AMD and the developed sensor were applied to control the vibration of a model structure with one DOF (one-degree-of-freedom).

For applying the AMD to these houses, cost-restriction is an important problem. Although acceleration sensors are commonly used for controlling vibration of high-rise buildings, this sensor needs high performance integrators with lower drift for obtaining the absolute displacement of the control object. Therefore a sensing system becomes expensive. As the developed sensor does not have the drift problem, cost reduction is possible. An image of three story houses equipped with the AMD and developed sensor is illustrated in the left side of Fig. 13. For controlling the first vibration mode, a 1DOF model with mass, M , and stiffness, K , was constructed as shown in the right side of Fig. 13. The main parameters of the model structure were $M = 4000$ kg and $K = 2526$ kN/m, and therefore the first natural frequency was 4 Hz. The active mass of the AMD was 175 kg.

A controlled result of the model structure equipped with the AMD and the developed sensor is shown in Fig. 14. A resonant peak located at 4 Hz was well controlled. The drift problem was completely eliminated by the use of the developed sensor, because the integration circuit was in a closed loop system.

6. Conclusions

In this research, a seismometer type absolute displacement was developed in order to expand the

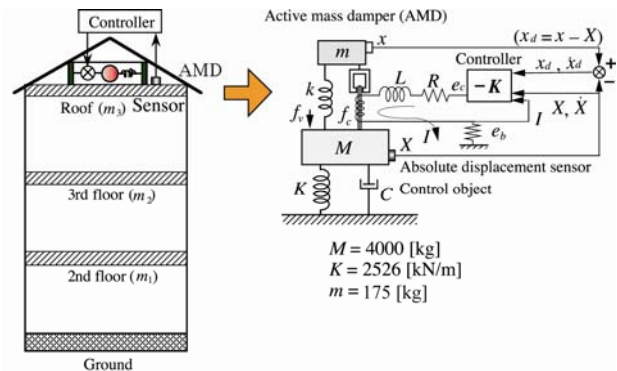


Fig. 13 Three story house equipped with the AMD and developed sensor.

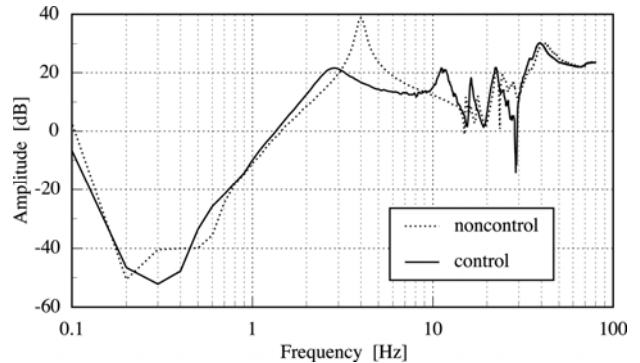


Fig. 14 Controlled result of the model structure with the AMD and developed sensor.

measuring-frequency range toward lower frequencies. A lower natural frequency of the sensor can be achieved using positive feedback from relative displacement and negative feedback from relative acceleration.

According to the simulation results, the natural frequency located at 5.5 Hz in the case of the original system is shifted to 0.7 Hz by the use of the all feedback (with positive displacement, negative acceleration and negative velocity gains) system, and is shifted still more to 0.2 Hz by phase-lag compensation. Furthermore, it is important to notice that the gain in measurement range was expanded from one of the original system to -40 dB = $1/100$ by use of negative acceleration feedback. This means that a small-size sensor with 1mm of moving distance allows a 100 mm measurement of the absolute displacement from a measured object.

The experimental result demonstrated that the developed sensor with a small size and lightweight has a detection range from 0.5 Hz to 50 Hz for the

absolute displacement. Although the frequency response indicated by the experimental results were not improved at the frequency range under 0.5 Hz, it will be improved by magnetic shielding from the electromagnetic shaker to the sensor, because induction from the shaker to the sensor is very sensitive under the lower frequency range with a feeble signal. If the frequency response of the phase angle is 180° below 1 Hz, it is possible to realize the frequency response indicated by the thick line in Fig. 5.

Two application examples such as seismic observations, active vibration controls for flexible structures were demonstrated by the use of the developed sensor. It was demonstrated that the drift problem has been completely eliminated by the use of the developed sensor.

References

- [1] B. F. Spencer and M. K. Sain, Controlling buildings: A new frontier of feedback, *IEEE Control System* 17 (6) (1997) 19–35.
- [2] K. Seto, Control of vibration in civil structures (Part 1), *Journal of Systems and Control Engineering* 218 (2004) 515–525.
- [3] F. S. Tse, I. E. Morse and R. T. Hinkle, *Mechanical Vibrations*, Prentice-Hall, 1963, pp. 78–81.
- [4] Y. Gatade, F. Doi and K. Seto, Development of an absolute displacement sensor for active vibration control, in: *Proceedings of Motion and Vibration Control in Mechatronics*, 1999, pp. 244–249.
- [5] T. Ishihara, T. Watanabe and K. Seto, Development of seismic type sensor for vibration control, in: *Proceedings of the 8th International Conference on Motion and Vibration Control (MOVIC)*, Daejeon Korea, 2006. [CD-ROM]
- [6] S. Wakui, D. Kojima and Y. Negishi, Realization of displacement sensor using calibration coil, *Journal of the Japan Society of Precision Engineers* 73 (3) (2007) 391–397.
- [7] F. Doi, Y. Gatade and K. Seto, Structural vibration control for bridge tower model using a new servo-type vibration sensor (Vol. 2), in: *Proceedings of Second World Conference on Structural Control*, 1998, pp. 1339–1347.
- [8] B. C. Kuo, *Automatic Control Systems*, Prentice-Hall, Inc, 1962, pp. 334–349.
- [9] S. Wakui, T. Kai and D. Kojima, Wide bandwidth of absolute velocity/displacement sensors and its application to vibration isolation table, *Journal of the Japan Society of Precision Engineers* 75 (4) (2009) 561–566.
- [10] K. Seto, *Vibration control of structure*, Corona Publishing Co., Ltd., 2006.
- [11] K. Seto, F. Doi and M. Ren, Vibration control of bridge towers using a lumped modeling approach, *Trans. of ASME, J. of Vibration and Acoustics* 121 (1999) 95–100.